

Chapter 4

Simulations in the Los Angeles Basin

This chapter reports the responses of steel moment-resisting frame (MRF) buildings to simulated earthquakes in the Los Angeles basin. I use broadband ground motions from simulations on the Puente Hills fault to compare the responses of shorter and taller steel MRF buildings. The taller buildings are more likely to collapse because they cannot sustain the large inter-story drifts induced in the lower stories. That is, the P- Δ effect affects taller buildings more than shorter buildings.

I also compare the building responses in several simulations of a large earthquake on the Puente Hills fault from two groups of researchers. The predicted building response at a single site can be sensitive to the particular assumed earthquake. However the regional response is similar for Puente Hills earthquakes of similar magnitude. There is general agreement on the effect of an earthquake of approximately magnitude 6.7 or 7.1 in the Los Angeles basin as a whole, despite local uncertainties in building response due to the specifics of the simulation.

The last section of this chapter discusses the utility of multiple simulations of the same magnitude earthquake on the same fault. The resulting building responses from repetitions of the “same earthquake” are quite similar, in terms of both regional extent of large building deformation and response as a function of peak ground velocity (PGV). Multiple simulations characterize the uncertainty in building response due to different rupture models of the same magnitude and fault configuration.

4.1 Ground Motion Studies

Porter et al. (2007) generated ground motions from scenario ruptures on the Puente Hills fault for the California Earthquake Authority. They used deterministic and stochastic models to generate broadband ground motions for periods greater than 0.1 s (Graves and Pitarka, 2004). In the study, the authors simulated a magnitude 7.15 earthquake with five distinct rupture models, varying the rupture speed, rise time, and slip distribution. Figure 4.1 maps the assumed fault and locates the hypocenter. For consistency, I follow the simulation numbering scheme in Porter et al. (2007). Figure 4.2 shows the broadband peak ground displacements (PGD_{bbs}) and peak ground velocities (PGV_{bbs}) for two of the simulations. Again, I measure the PGD and PGV as the largest vector amplitude from the two horizontal, north-south and east-west components of ground motion.

As part of the Pacific Earthquake Engineering Research Center Lifelines program, several groups of Southern California Earthquake Center researchers developed models to generate ground motions in the Los Angeles basin (Day et al., 2001, 2003, 2005). The stated purposes of the studies were to: validate wave propagation models and algorithms with simple and complex earthquake sources and earth structures; characterize the amplification of long-period waves due to sedimentary basins; and archive the ground motions for future engineering studies. They generated long-period ground motions for sixty scenario earthquakes on ten known faults or fault systems in the Los Angeles basin. For each fault in the study, the researchers generated three slip distributions and assumed two hypocenter locations for each slip distribution. The hypocenter locations are relatively deep on the fault (at a distance 0.7 of the fault width as measured from the top of the fault along the dip), and the ruptures propagate up-dip. If the authors had assumed shallow hypocenters and down-dip ruptures instead, the peak ground displacements and velocities would have been smaller (Aagaard et al., 2004).

Table 4.1 lists the scenario earthquakes used in this thesis, and Figure 4.3 locates the faults. Figure 4.4 shows the long-period peak ground displacements and velocities

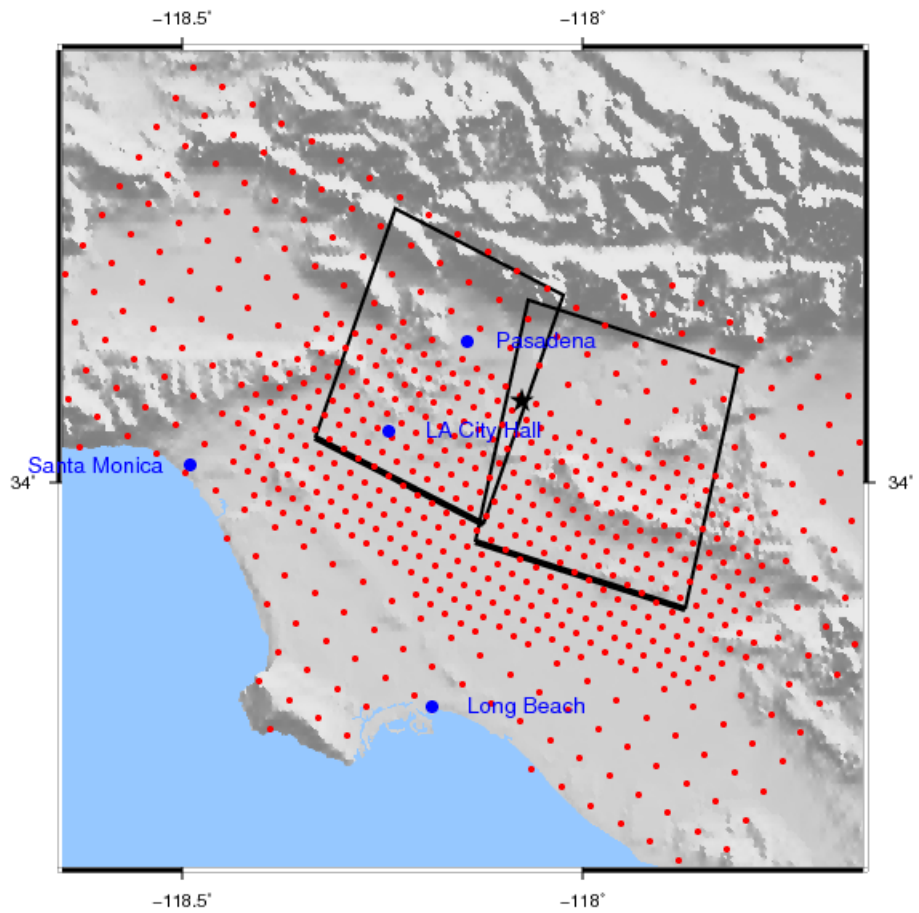


Figure 4.1: The Porter et al. (2007) simulation domain covers the Los Angeles, San Fernando, and San Gabriel basins in the Los Angeles area. Red dots locate the 648 sites in the domain, and blue dots locate major cities in the area. The black lines outline the assumed fault segments, and the black star locates the hypocenter.

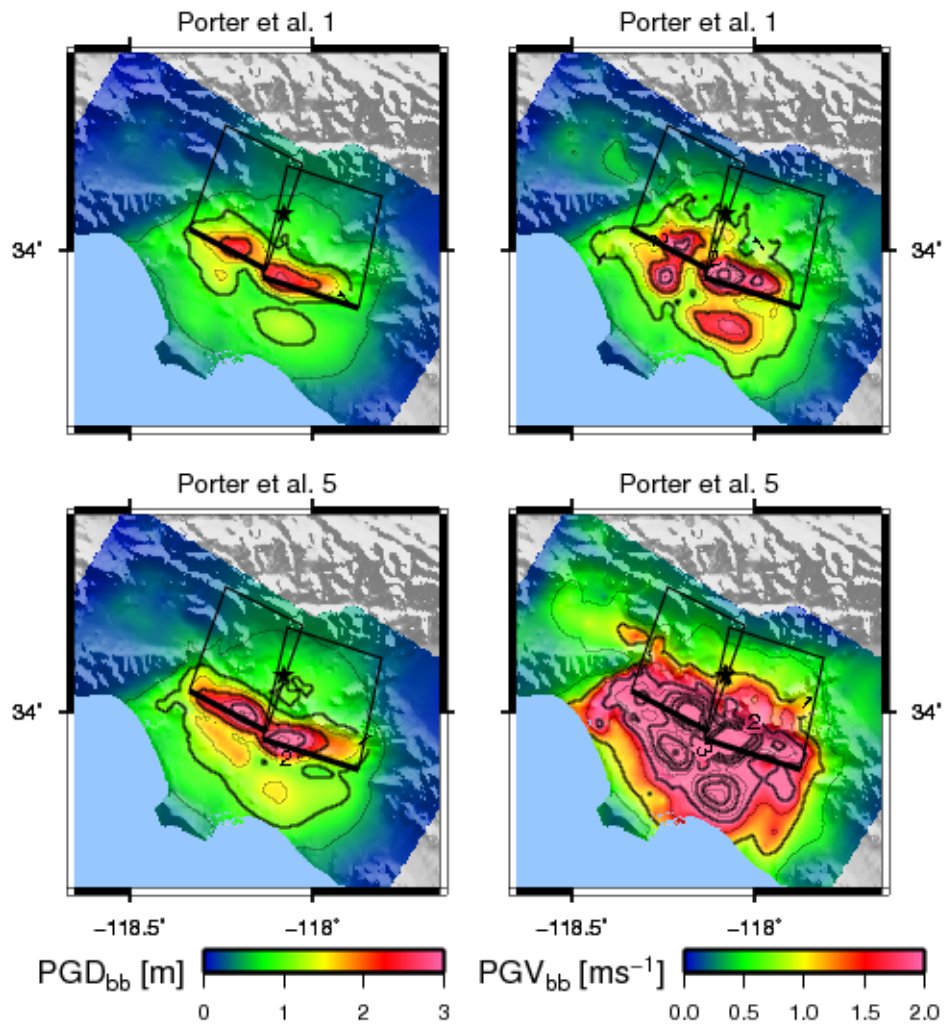


Figure 4.2: Porter et al. (2007) generated five magnitude 7.15 simulated earthquakes on the Puente Hills fault. This figure shows the broadband PGD and PGV for two of these simulations. Simulation 1 (top maps) is representative of the ground motion for all five simulations, whereas simulation 5 (bottom maps) has the largest ground motions of all five simulations.

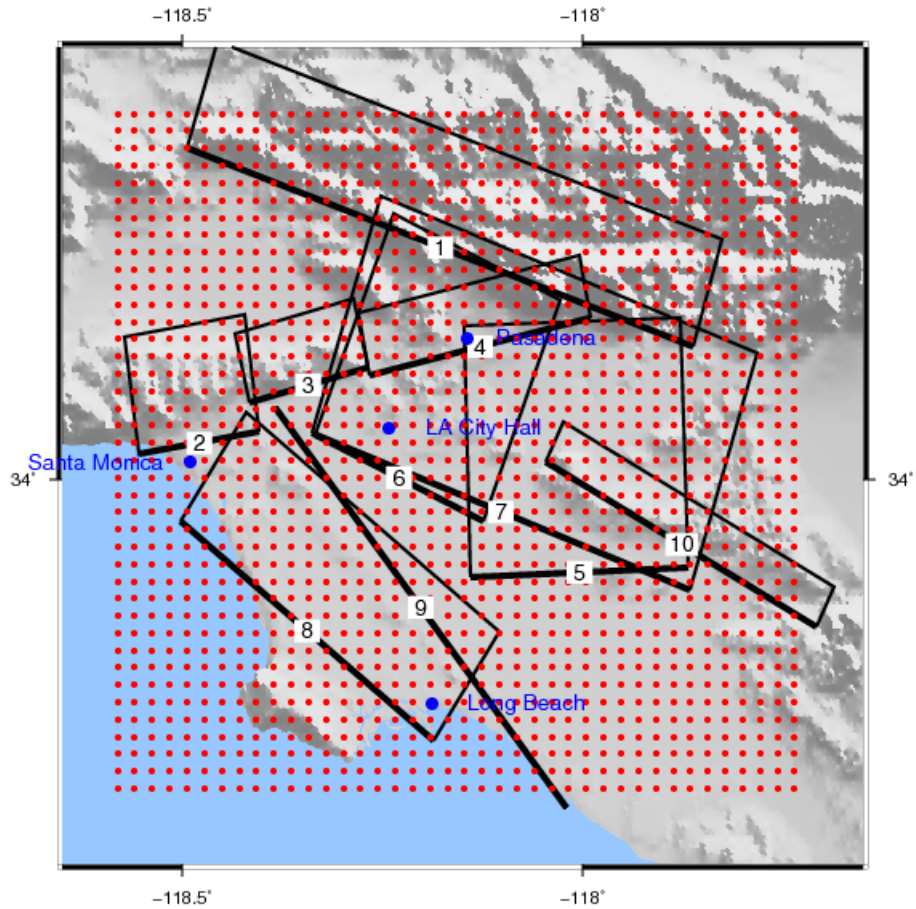


Figure 4.3: Day et al. (2005) simulated long-period ground motions in the Los Angeles basin. Red dots locate the 1600 simulation sites, and blue dots locate major cities in the area. There are simulated ruptures on the ten faults labeled here.

for two simulations.

4.2 Six- versus Twenty-Story Building Responses

Since the Porter et al. (2007) broadband ground motions have energy content in the range of the fundamental periods of both the six- and twenty-story building models, I can compare the responses of the two building heights. Figure 4.5 graphs the peak IDRs for the six- and twenty-story models. Generally, the twenty-story models do not sustain a peak IDR more than 10%, whereas the six-story models sustain up to 16%, without collapsing. Figure 4.6 directly compares the responses of six- and twenty-

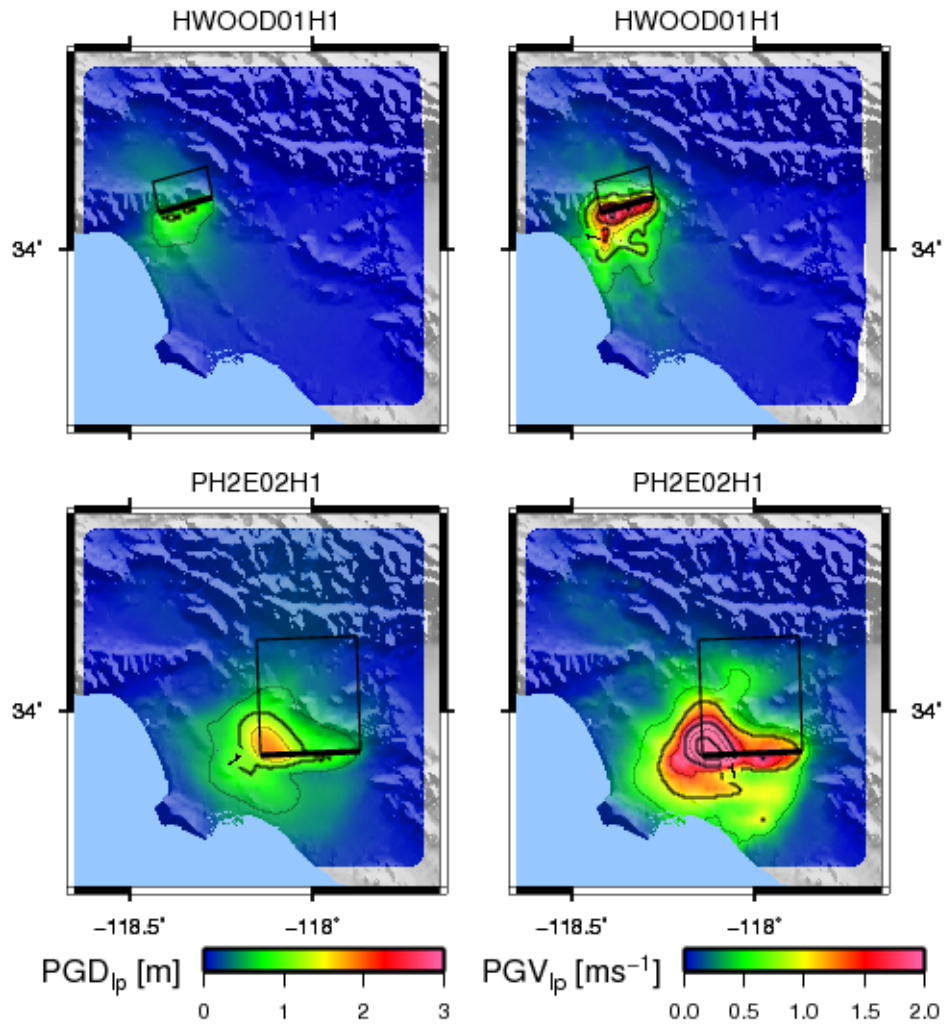


Figure 4.4: This figure shows the long-period PGD and PGV for two simulations in the Los Angeles Basin. The simulation on the Puente Hills fault (bottom maps) generates large ground motions in much of the Los Angeles Basin, whereas the simulation on the Hollywood fault (top maps) has large ground motions in the area above the top edge of the fault.

<i>Fault name</i>	<i>M</i>	<i>No.</i>	<i>Fault abbrev.</i>	<i>Slip code</i>	<i>Hypocenter code</i>
Compton	6.9	8	COMP	02	H1
Hollywood	6.4	3	HWOOD	02, 04, 06	H1, H2
Puente Hills (2 seg.)	6.8	5	PH2E	02, 05, 09	H1, H2
Puente Hills (3 seg.)	7.1	7	PHALL	02	H1
Puente Hills (1 seg.)	6.7	6	PHLA	01	H1
Newport-Inglewood	6.9	9	NIN	01	H1
Raymond	6.6	4	RAYM2	07	H1
Sierra Madre	7.0	1	SMAD	03	H1
Santa Monica	6.3	2	SMON	03	H1
Whittier	6.7	10	WHIT	01	H1

Table 4.1: This table lists the simulations of long-period ground motions in the Los Angeles basin used in this thesis. Consistent with Day et al. (2005), each scenario earthquake has a name concatenated from a code name, slip code, and hypocenter code. For example, a scenario rupture on the three segments of the Puente Hills fault system with slip distribution two and hypocenter one is coded PHALL02H1.

story models at the same site for all ground motions in the five simulated earthquakes. For three of the building models (the stiffer, higher-strength with perfect and brittle welds (JP and JB) and the more flexible, lower-strength with brittle welds (UB)) the twenty-story building collapses on a greater proportion of sites than does the six-story building. The six-story, more flexible, lower-strength building with perfect welds (U6P) collapses on a greater proportion of sites than does the equivalent twenty-story building (U20P). Assuming both the six- and twenty-story buildings stand at a site, the peak IDR in the six-story building is approximately 1.2–1.6 times that of the twenty-story building, depending on the design and weld state. Thus, in general, the twenty-story building is more likely to collapse than the six-story building (due to P- Δ effects), but if buildings of both heights remain standing at a site, then the peak IDR in the six-story building is larger than the peak IDR in the twenty-story building.

Building height seems not to affect the propensity of a *properly designed and constructed* steel MRF to collapse. For the stiffer, higher-strength building with perfect welds (JP), the twenty-story building is somewhat more likely to collapse than the equivalent six-story building. However, for the more flexible, lower-strength building with perfect welds (UP), the six-story building is somewhat more likely to collapse

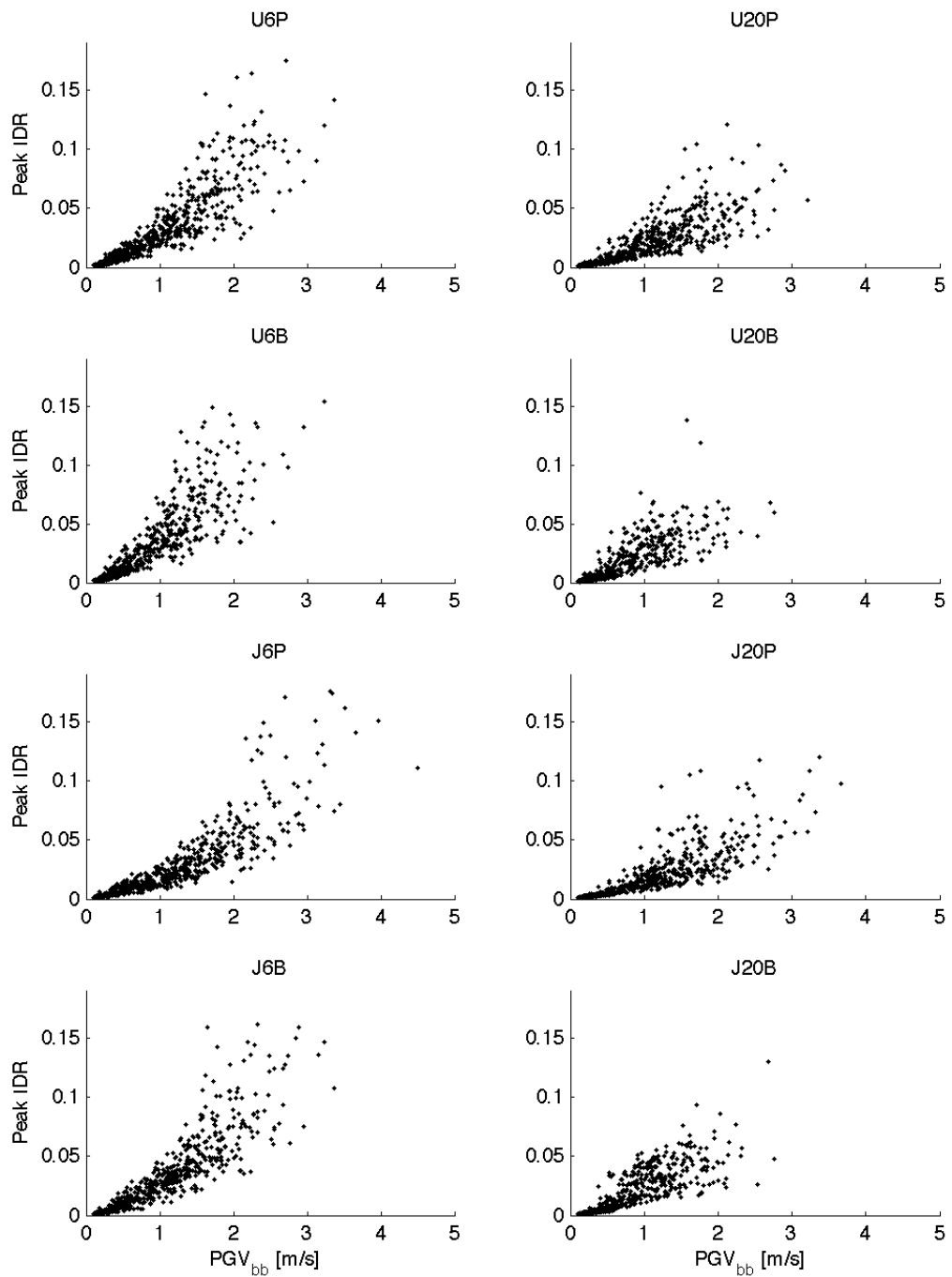


Figure 4.5: In the simulations, six-story building models remain standing with up to 16% peak IDR whereas twenty-story models sustain peak IDRs up to 10%. Since the largest peak IDRs tend to localize in the first few stories, the eccentric gravity load of a twenty-story building is more likely to overcome the moment-resisting capacity of the columns in the lowest stories. Thus, the twenty-story building is more likely to collapse at lower peak IDRs. The data in this figure are from building responses in the Porter et al. 2 simulation.

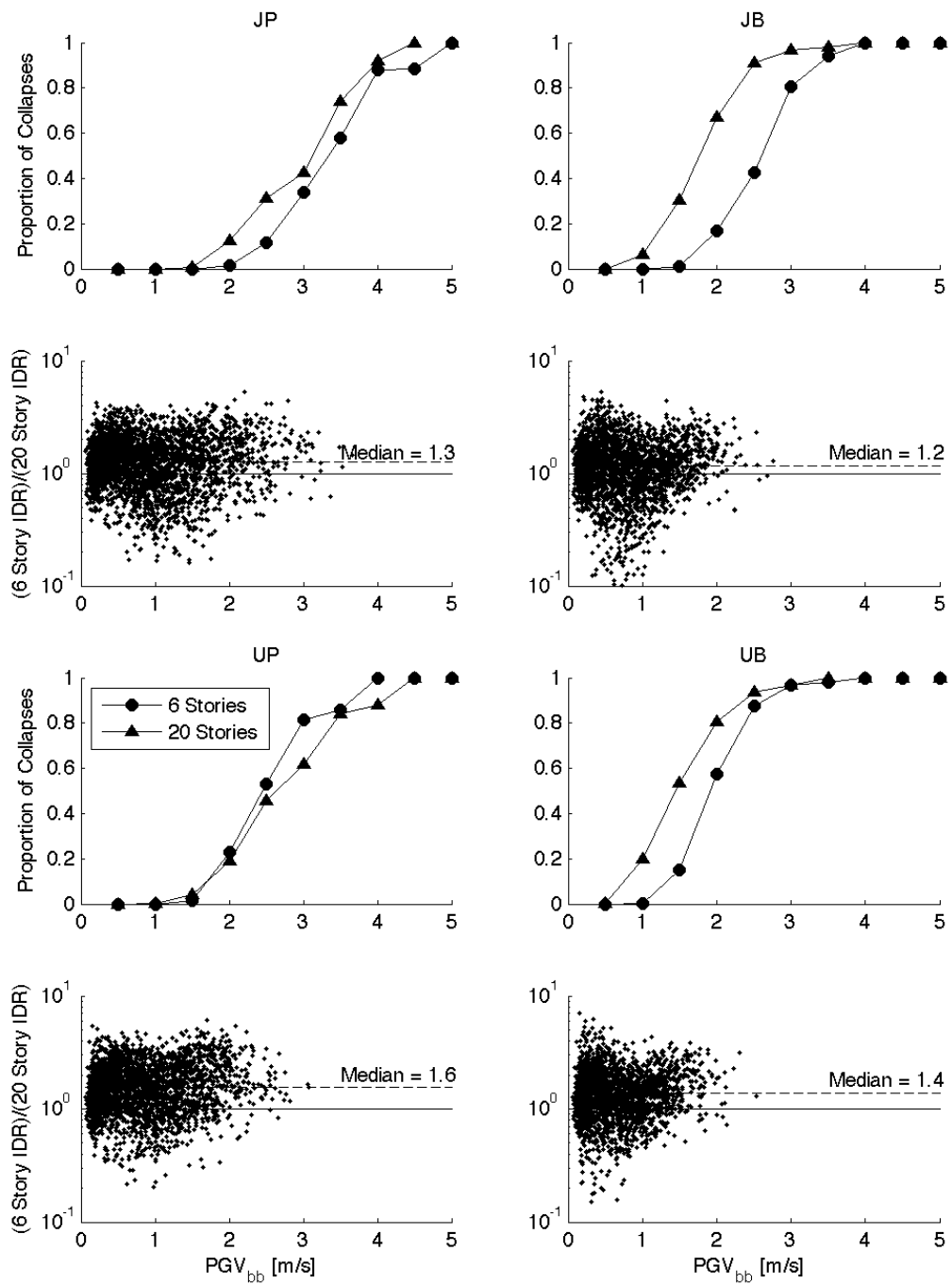


Figure 4.6: For models with perfect welds (graphs on left), the six- and twenty-story buildings have a similar number of collapses. However, if the models have brittle welds (graphs on right), the twenty-story building is much more likely to collapse while the six-story stands. If both buildings remain standing at a site, then the peak IDR of the six-story building is likely 1.2–1.6 times the peak IDR of the twenty-story building, depending on the design and weld state. The data in this figure are from building responses in the five magnitude 7.15 simulations on the Puente Hills fault in Porter et al. (2007).

than the equivalent twenty-story. This result makes sense because engineers assume a seismic hazard and accordingly design buildings to remain standing in ground motions consistent with that hazard. The additional moment induced in the columns of the lowest stories from an eccentric vertical load (that is, the P- Δ effect) is well known. Designs of taller buildings account for this effect.

The presence of brittle welds makes the taller designs more vulnerable to collapse than the six-story buildings. For both the stiffer and more flexible designs, the twenty-story building is much more likely to collapse in a ground motion with a given peak ground velocity than the equivalent six-story building. Obviously the presence of brittle welds significantly degrades the lateral force-resisting capacity of both story heights, but the consequence is much more severe for the twenty-story buildings.

The problem of brittle welds could also be considered as an example of an unknown design or construction flaw. Taller buildings tend to be inherently more unstable than equivalent shorter buildings. An unanticipated flaw makes buildings of both heights even more unstable, especially if buildings of both heights are vulnerable at their bases. Using brittle welds as an example, design and construction flaws make taller buildings more vulnerable to collapse than shorter buildings.

4.3 Puente Hills Fault Simulations

This thesis includes several simulated earthquakes on the Puente Hills fault system. Day et al. (2005) hypothesized three earthquakes that rupture one (magnitude 6.7, PHLA), two (magnitude 6.8, PH2E), or three segments (magnitude 7.1, PHALL) of the fault system. Figure 4.7 maps the twenty-story, more flexible, lower-strength (U20P) building responses to these simulations as well as the responses to one of the Porter et al. (2007) simulations. The areal extent of inelastic building responses (colored green to pink) is similar between the magnitude 6.7 and 6.8 ruptures and between the magnitude 7.1 and 7.15 ruptures. Also the total area of the largest building responses (peak IDR greater than 0.05, colored red to pink) is similar within the two sets of magnitude. However the particular locations of these areas are different

among the two sets.

The magnitude 6.7 and 6.8 simulations (top subfigures) show similar results in the Los Angeles basin: there is a limited area of large peak IDRs in the vicinity of the projected top edge of the fault plane, and the building response over much of the Los Angeles basin is inelastic. The rupture on the Los Angeles segment (top-left subfigure) causes inelastic building responses mostly in the central and western parts of the Los Angeles basin, whereas the rupture on the Santa Fe and Coyote Hills segments (top-right subfigure) causes inelastic responses in the central and eastern portions. This difference is due to the orientation of the fault plane and particular combination of slip distribution and rupture propagation. It is independent of the particular rupture and building model.

Likewise the magnitude 7.1 and 7.15 simulations (bottom subfigures) show similar results: the areas of large peak IDRs cover most of the Los Angeles basin, and the building responses in the entire Los Angeles basin are inelastic. The magnitude 7.1 rupture (bottom-left subfigure) has two distinct areas of large peak IDRs: one area is due south of the southeast fault corner, in the easternmost portion of the basin; and the second area is west and south of the southwest fault corner, in the northwest part of the basin. The magnitude 7.15 rupture (bottom-right subfigure) induces large peak IDRs in the areas above and just south of the projected top edge of the fault plane. This difference in the location of the largest peak IDRs is due to the relative locations of the hypocenter and large patches of slip on the fault plane. The location of the largest peak IDRs is coincident with the location of the largest peak ground displacements and velocities.

Figure 4.8 graphs the building responses in these four Puente Hills earthquakes. Again, the data are consistent within the smaller and larger magnitudes. Buildings in the smaller simulations (magnitude 6.7 and 6.8) collapse on similar proportions of sites with a given PGV_{ip} . If the buildings do not collapse, then buildings in the magnitude 6.7 simulation tend to have smaller peak IDRs compared to the other Puente Hills simulations. Buildings in the larger simulations (magnitude 7.1 and 7.15) collapse on similar proportions of sites for PGV_{ip} s less than 1.5 m/s, but they differ for larger

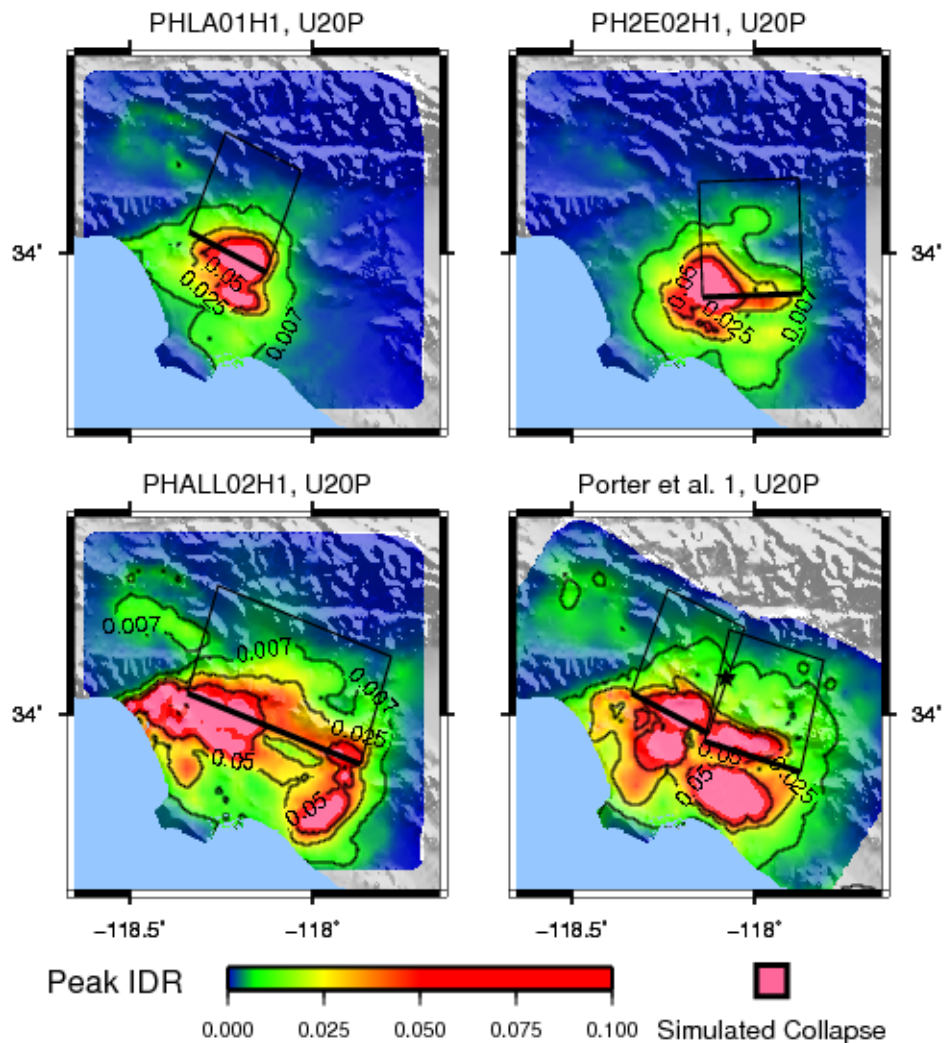


Figure 4.7: This figure compares the U20P building model responses in four simulations on the Puente Hills fault in the Los Angeles area. A magnitude 6.7 or 6.8 earthquake (top left and right maps, respectively) causes inelastic building response on most of the Los Angeles basin with the largest peak IDR (greater than 0.05) in the vicinity of the top edge of the fault. A magnitude 7.1 or 7.15 earthquake (bottom left and right maps, respectively), however, induces inelastic building responses on the entire Los Angeles, San Fernando, and San Gabriel basins, with extensive areas of large peak IDRs in the Los Angeles basin. Note the general similarity in the magnitude 7.1 simulations even though they were provided by two separate research groups.

PGV_{ip}s. The proportion of collapses continues to rise with increasing PGV_{ip} for the magnitude 7.15 simulation (Porter et al. 1), but it levels off, and somewhat declines, for the magnitude 7.1 simulation (PHALL02H1). The PHALL02H1 curve has insufficient data to properly characterize the proportion of collapse (Section 4.4). The symbol at PGV_{ip} \approx 2 m/s represents 24 data points, PGV_{ip} \approx 2.5 m/s represents 6 data points, and PGV_{ip} \approx 3 m/s represents 1 data point. Nonetheless, both large magnitude simulations generate larger peak IDR compared to the smaller magnitude simulations, suggesting there may be a magnitude dependence not considered in this thesis.

4.4 Multiple Simulations of the Same Earthquake

I simulated the responses of the building models for multiple simulations of the same earthquake. Day et al. (2005) and Porter et al. (2007) generated several source models for the same magnitude earthquake on the same fault. These multiple simulations explore the uncertainty inherent in modeling an earthquake. Defining an earthquake simply by magnitude and fault is an ill-posed problem. Many combinations of slip pattern on the fault and rupture characteristics produce the “same earthquake.” Multiple simulations give an idea of the sensitivity of the building responses to the simulation. One simulation may not be sufficient to probabilistically model building response in a simulation.

Figures 4.9–4.11 map the twenty-story, more flexible building (U20P) responses to five or six multiple simulations on the same fault. Within each set of building responses, the areal extents of inelastic and collapsed building responses are similar, but there are differences at individual sites. For the ruptures on the Hollywood fault (Figure 4.9), the patterns of building response in the Los Angeles basin are quite similar. For the magnitude 6.8 ruptures on the Puente Hills fault (Figure 4.10), the locations of building collapses differ: there are consistently many collapses above the

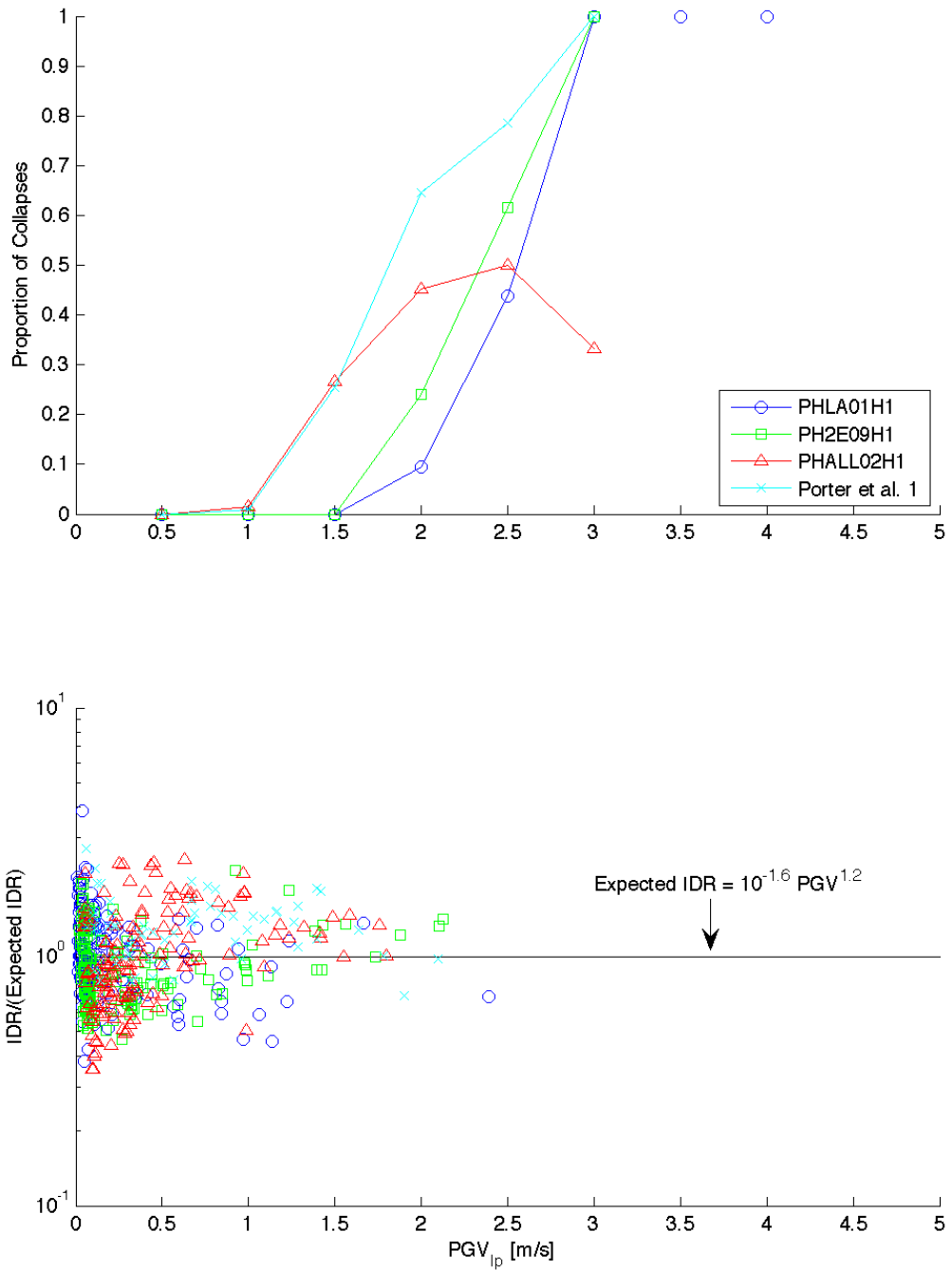


Figure 4.8: This figure compares the collapse and peak IDR responses of the U20P model in four Puente Hills fault simulated earthquakes. The smaller earthquakes (magnitude 6.7 PHLA01H1 and magnitude 6.8 PH2E09H1) have consistent proportions of collapse as functions of long-period peak ground velocity. The proportions of collapse of the larger earthquakes (magnitude 7.1 PHALL02H1 and magnitude 7.15 Porter et al. 1) are consistent for PGV_{ip} less than 2 m/s. The PHALL02H1 curve levels off and declines for PGV_{ip} greater than 2 m/s due to insufficient data at these large intensities to properly characterize the curve.

top edge of the fault, but south of that area, there may or may not be a second area of collapses, depending on the simulation. For the magnitude 7.15 ruptures on the Puente Hills fault (Figure 4.11), the first three simulations show stable patterns of building response, whereas simulation 4 causes collapses on a smaller area and simulation 5 induces collapses on a larger area. These three figures show that a single simulation of an earthquake may be appropriate to get a sense of the regional extent of building responses, but multiple simulations may be necessary to adequately characterize, in a probabilistic manner, the expected ground motion at a specific site.

Figures 4.12–4.14 graph the building responses as functions of peak ground velocity. The relationship between collapse and peak ground velocity is not well defined if there is not sufficient data. The simulations on the Hollywood fault (Figure 4.12) do not generate enough large ground motions to accurately characterize what proportion of buildings collapse at a given PGV_{lp} . For PGV_{lp} greater than 2.5 m/s, there are fewer than four data points for each PGV_{lp} level in each simulation. The suspicious results in Figure 4.12 are due to this lack of data. The simulations on the Puente Hills fault have enough strong ground motions to produce consistent relationships between collapse and peak ground velocity (Figures 4.13 and 4.14). For the two sets of simulations on the Puente Hills fault, there is much more agreement within each set compared to the set on the Hollywood fault. However, within the two Puente Hills sets, there is still uncertainty in the proportion of collapse at a given peak ground velocity. For example, the PH2E02H1 simulation shows 100% collapse of the U20P model for PGV_{lp} approximately 2.5 m/s, compared to 30% in the PH2E09H2 simulation. The building responses in a single simulation are not adequate to characterize the uncertainty in building response as a function of peak ground velocity.

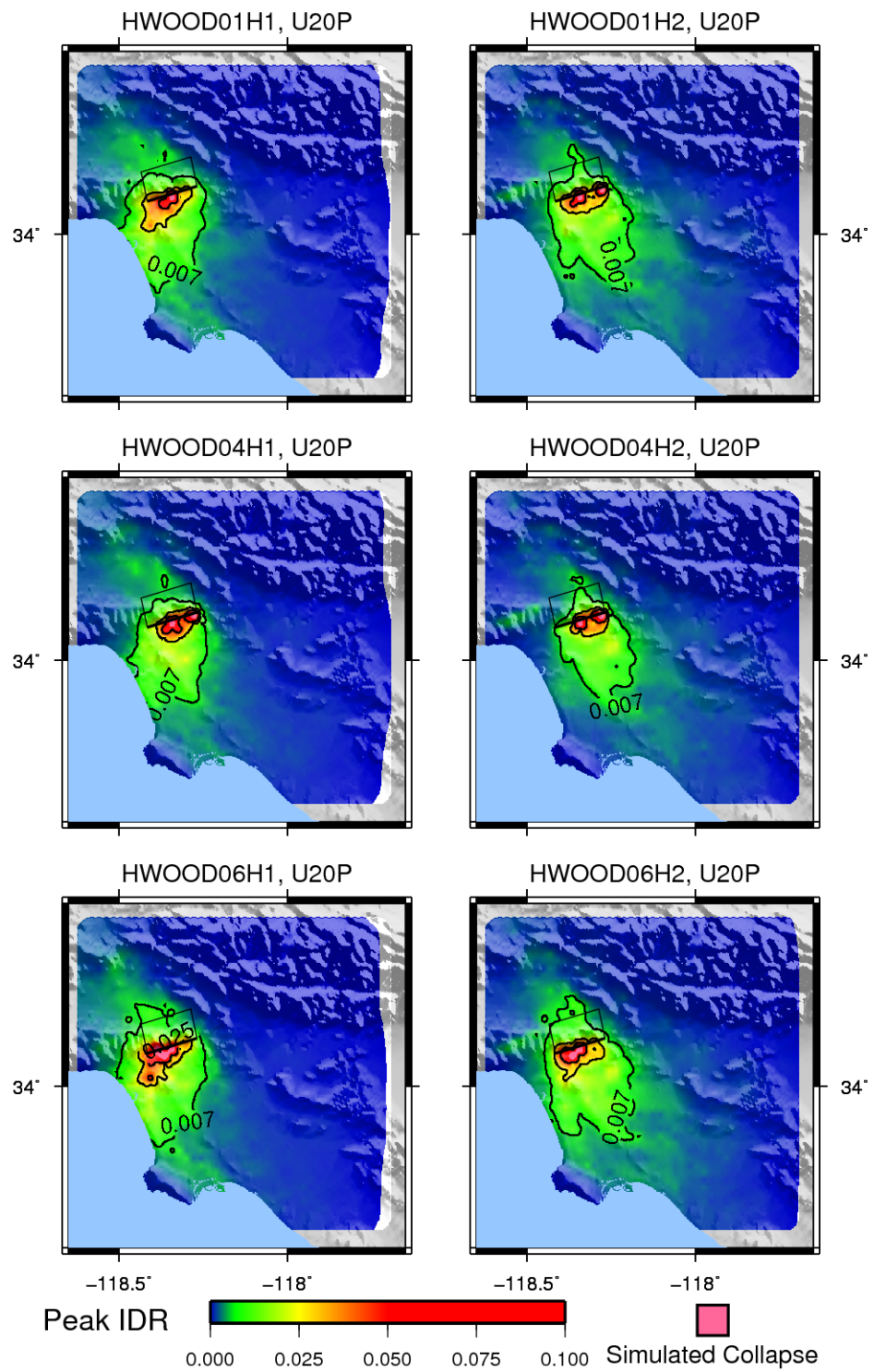


Figure 4.9: This figure maps the responses of the U20P model in multiple realizations of a magnitude 6.4 earthquake on the Hollywood fault.

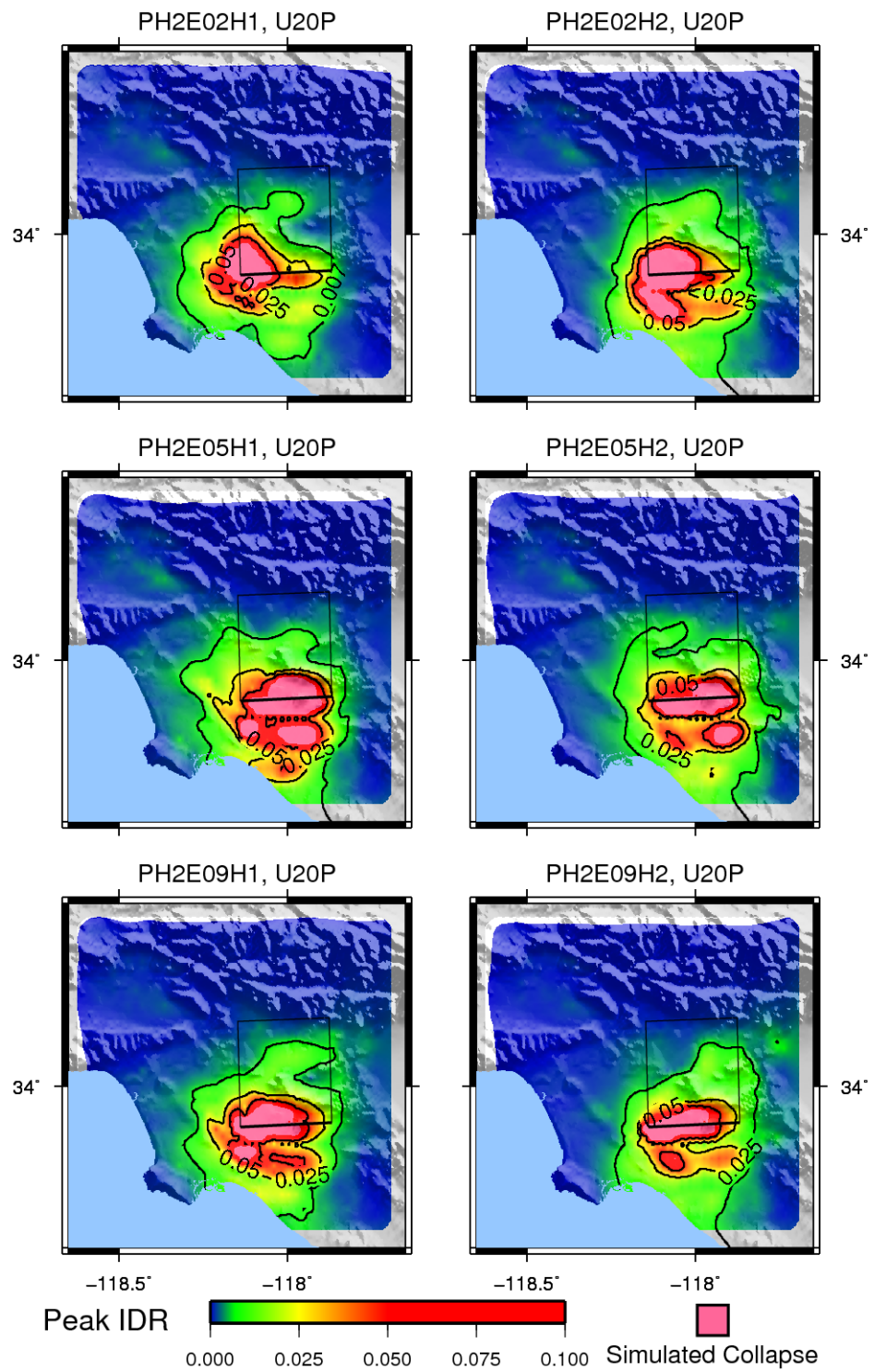


Figure 4.10: This figure maps the responses of the U20P model in multiple realizations of a magnitude 6.8 earthquake on the Puente Hills fault.

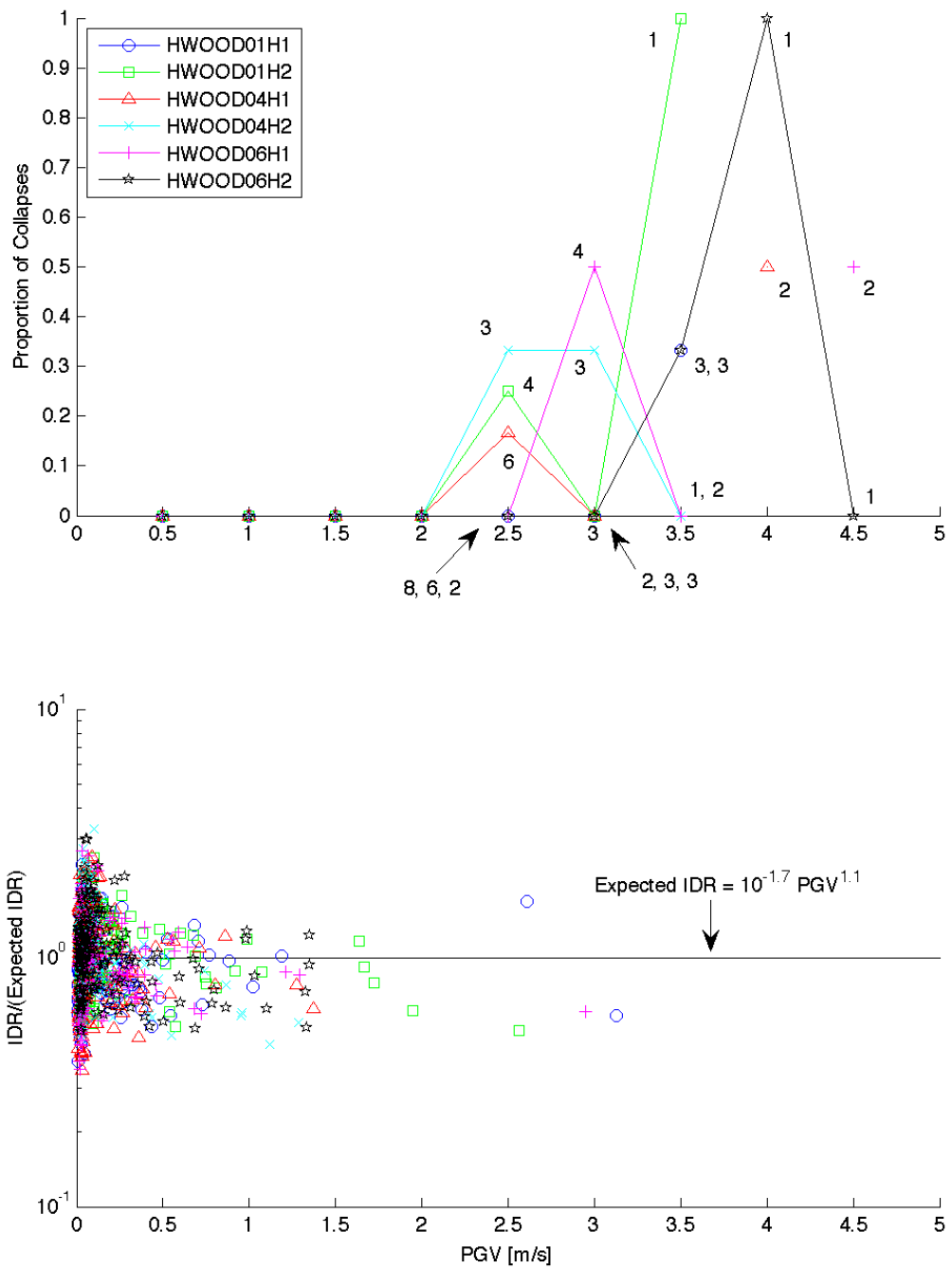


Figure 4.12: This figure compares the responses of the U20P model in multiple realizations of a magnitude 6.4 earthquake on the Hollywood fault. The numbers beside the symbols indicate the amount of data represented by that point. Note the scarcity of data for PGV_{Ip} greater than 2.5 m/s.

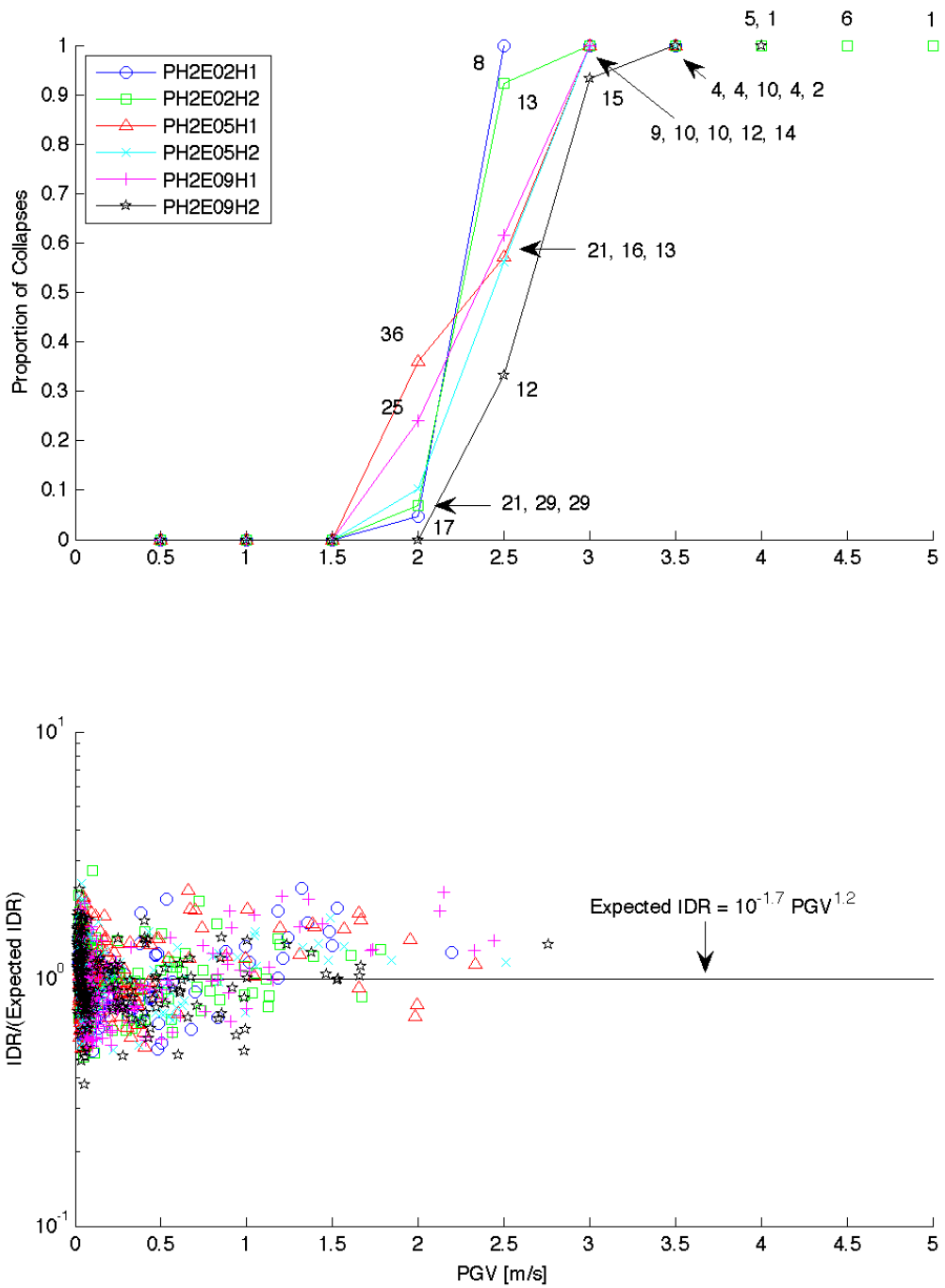


Figure 4.13: This figure compares the responses of the U20P model in multiple realizations of a magnitude 6.8 earthquake on the Puente Hills fault. The numbers beside the symbols indicate the amount of data represented by that point. There is more available data for PGV_{lp} greater than 2.5 m/s, compared to the data from the Hollywood fault. Thus, the probability of collapse is well defined and consistent for all six realizations.

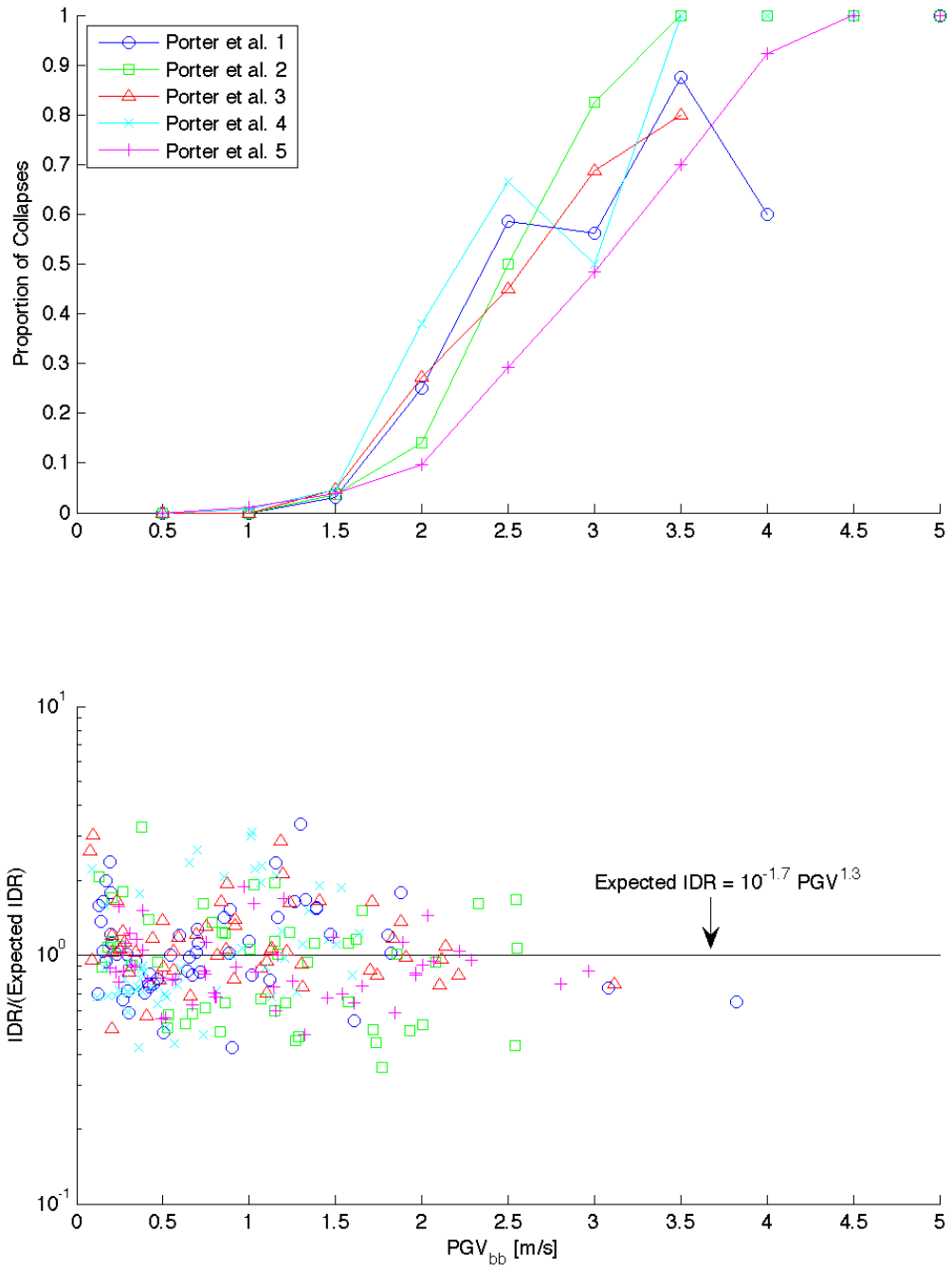


Figure 4.14: This figure compares the responses of the U20P model in multiple realizations of a magnitude 7.15 earthquake on the Puente Hills fault. The building responses are consistent for these five realizations.